AIAA JOURNAL
Vol. 38, No. 7, July 2000

Unsteady Swirling Flows in Annular Cascades, Part 1: Evolution of Incident Disturbances

Vladimir V. Golubev* and Hafiz M. Atassi†
University of Notre Dame, Notre Dame, Indiana 46556

A theory is developed for the interaction of an unsteady incident disturbance with an annular cascade in a mean swirling flow. It is shown that the centrifugal and Coriolis forces caused by the mean swirl couple the acoustic and vortical disturbance modes and can lead to the formation of a critical layer. A normal mode analysis shows that, for moderate subsonic Mach numbers, the eigenmodes, which may not form a complete set, are segregated into pressure-dominated and vorticity-dominated modes. A complete description of incident disturbances is proposed in terms of the pressure-dominated eigenmodes and a spatially developing initial-value solution. For the special case of a potential mean swirl, the vortical modes are uncoupled from the acoustic modes, and their vorticity grows linearly as they propagate downstream. For a general vortical mean swirl the vorticity-dominated spatially developing disturbances may oscillate or amplify (decay) depending on the radial distribution of the mean swirl. The analysis clearly indicates a significant effect of the mean-flow swirl on the evolution of the incident disturbances and therefore on the blade upwash.

Introduction

THE interaction of flow nonuniformities with turbomachinery blading systems produces fluctuating forces along the blades and results in unwanted effects such as noise and forced vibration. Most analyses of these unsteady flow phenomena follow external unsteady aerodynamic theory, where the unsteady flow is linearized about a mean flow with uniform upstream conditions; thus, the impinging nonuniformities are imposed upstream on a uniform mean flow. It is then possible to split these disturbances into distinct potential, entropic, and vortical modes obeying independent equations and to study their interaction with the downstream blades.[1]

The assumption of an upstream uniform flow is adequate for inlet distortions provided the entire rotor/stator system is coupled together. However, accurate resolution of the unsteady aerodynamics and acoustics of a coupled rotor/stator system remains a formidable computational problem. The problem is simplified by considering separately each blade row and imposing upstream disturbances on its mean flow to account for the effects of the wakes and secondary flows. In turbomachines interstage mean flows have a significant swirl velocity whose magnitude may be equal to that of the axial velocity. Thus wake and secondary flows nonuniformities must be imposed on a swirling motion. The mean swirl produces centrifugal and Coriolis forces causing a force imbalance that deflects the fluid motion and couples the vortical, entropic and acoustic modes.[2]

The effects of the mean swirl on the unsteady eigenmodes propagating in annular duct have been studied by Golubev and Atassi.[3,4] Their results show that, at moderate subsonic Mach numbers, there are two distinct sets of eigenmodes. One set represents nearly sonic pressure-dominated modes with small vorticity associated with them. The other set represents nearly convected vorticity-dominated modes with small pressure content. For the pressure-dominated modes the effect of the mean swirl is to modify the impedance of the system by modifying mainly the cut-on frequencies. On the other hand, the vorticity-dominated modes have, in general, eigenvalues that accumulate with increasing density near the edges of a critical layer. Moreover, because the boundary-value problem describing the modes is not self-adjoint, the eigenmodes may not form a complete set.

To avoid these difficulties and to describe the most general vortical and acoustic disturbances, we propose to combine the eigenmode analysis with an initial-value analysis to account for the effects of spatially developing disturbances that evolve as they propagate and that may not be accounted for by the eigenmode analysis. Despite the modal coupling, it is convenient to decompose the disturbance velocity field into vortical and potential parts. Such decomposition has the advantage of elucidating the physical phenomena associated with unsteady motion by indicating the degree of interaction between the various modes. It also paves the way to extending the classical definition of a gust to vortical swirling flows.

For simplicity, we consider the mean flow velocity to be composed of an axial velocity, a potential free-vortex rotation, and a vortical rigid-body rotation. We further assume the stagnation enthalpy of the mean flow to be constant. The mean swirl can then be characterized in terms of two parameters representing the strength of the free vortex Γ and the rigid-body angular velocity Ω. We first consider the case of a potential mean flow ($\Omega = 0$), where it is possible to partially split the unsteady velocity field into vortical and potential parts. The vortical part can be uncoupled from the potential part, and its expression can be derived analytically.[5,6] Such a solution corresponds to the continuum convected spectrum of radial modes in the eigenmode analysis.[4] The potential part, which depends on the vortical solution, is governed by an inhomogeneous nonconstant coefficient convected wave equation.

In the general case of a vortical swirl, the potential and vortical parts of the unsteady velocity are mutually coupled by the mean-flow vorticity. However, the eigenmode analysis in Ref. 4 reveals that, for moderate subsonic Mach numbers, this coupling is weak as two distinct regions of eigenvalues appear corresponding to pressure-dominated nearly sonic eigenmodes and vorticity-dominated nearly convected eigenmodes. A combined eigenmode and initial-value analysis is then developed to represent the most general upstream disturbances. The pressure-dominated eigenmodes represent the acoustic part of the solution, whereas the initial-value solution represents the vorticity-dominated nearly convected eigenmodes. The results indicate that the initial-value solution, which may represent decaying, propagating, and amplifying modes, has a significant effect on the total unsteady velocity.

Formulation

The present analysis is aimed at calculating the unsteady response of an annular unloaded subsonic cascade due to its interaction with unsteady, inviscid, compressible swirling flow, as illustrated in Fig. 1. The annulus is considered with constant hub and tip radii r_h and r_t.

Received 5 April 1997; presented as Paper 97-1635 at the 3rd Joint CEAS/AIAA Aeroacoustics Conference, Atlanta, GA, 12–14 May 1997; revision received 13 September 1999; accepted for publication 15 September 1999.

*Research Associate, Department of Aerospace and Mechanical Engineering. Member AIAA.

†Viola D. Hank Professor, Department of Aerospace and Mechanical Engineering. Fellow AIAA.

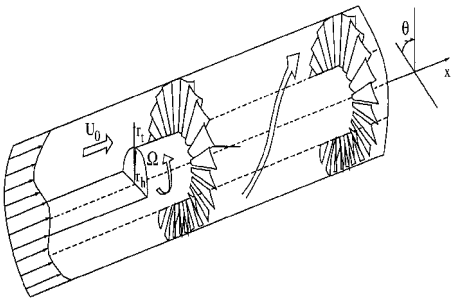

Fig. 1 Unsteady annular cascade swirling flow.

The assumption is further made that the flow unsteady velocity part represents a small-amplitude perturbation of the total mean swirling flowfield, and thus the total flow velocity may be decomposed as follows:

$$\boldsymbol{V}(\boldsymbol{x}, t) = \boldsymbol{U}(\boldsymbol{x}) + \boldsymbol{u}(\boldsymbol{x}, t) \tag{1}$$

with the general form of the mean swirling velocity profile

$$\boldsymbol{U}(\boldsymbol{x}) = U_x \hat{e}_x + U_s \hat{e}_\theta \tag{2}$$

where $\hat{e}_x$ is the unit vector in the axial direction and $\hat{e}_\theta$ is the unit vector in the circumferential direction. The corresponding mean velocity components U_x and U_s can vary with radius r (the latter and all lengths are normalized throughout the paper by the mean radius of the annulus r_m). The mean-flow model adopted in the present analysis is based on typical turbomachinery design conditions described next.

Mean-Flow Model

The mean annular cascade flow is assumed to be in a radial equilibrium state so that the radial mean pressure distribution is established to balance the centrifugal forces acting on a fluid particle. From Crocco's equation one can easily obtain the following relation between the mean-flow stagnation enthalpy h_0, temperature T_0, entropy S_0, and velocity $\boldsymbol{U}$:

$$\frac{\mathrm{d}h_0}{\mathrm{d}r} = T_0 \frac{\mathrm{d}S_0}{\mathrm{d}r} + U_x \frac{\mathrm{d}U_x}{\mathrm{d}r} + U_s \frac{\mathrm{d}U_s}{\mathrm{d}r} + \frac{U_s^2}{r} \tag{3}$$

The term $T_0(\mathrm{d}S_0/\mathrm{d}r)$ may be significant if the flow Mach number relative to the blade is supersonic and shock losses occur. In the present analysis the entropy gradients are neglected. Moreover, apart from regions near the walls of the annulus, the stagnation enthalpy and temperature are usually uniform across the annulus at the entry to an engine stage. However, after interacting with the first blade row, the enthalpy h_0 typically will depend on the radius r. In the present paper, for simplicity we assume the enthalpy h_0 to be constant. Thus, Eq. (3) reduces to

$$U_x \frac{\mathrm{d}U_x}{\mathrm{d}r} + U_s \frac{\mathrm{d}U_s}{\mathrm{d}r} + \frac{U_s^2}{r} = 0 \tag{4}$$

In turbomachinery design one may consider a special case when the axial velocity U_x remains constant across the annulus. Then, integrating Eq. (4) gives

$$U_s r = \text{const} \tag{5}$$

hence a free-vortex flow condition is obtained. In practice, there are certain disadvantages associated with a free-vortex blading,[7] one of them being a significant variation of the blade degree of reaction with radius given in terms of the enthalpy rise in the rotor (a measure of rotor contribution to the overall static pressure rise in the stage).

Other possible sets of mean-flow design conditions may involve variation of one of the velocity components, say U_s, and then determining the variation of U_x from Eq. (4). A general form studied in design applications[7] determines the swirl distribution at the inlet and outlet of the rotor stage in terms of the following law:

$$U_s = \Omega r^n \pm \Gamma / r \tag{6}$$

where Ω, Γ, and n are constants.

In the present analysis a special case of $n = 1$ is used to model the swirling component of the mean-flow velocity. This approach, based on the mean swirl representation with only two parameters Γ and Ω (describing a free-vortex and a rigid-body mean-flow rotations, respectively), is especially useful to develop physical insight into the problem. Thus, the total variation of the circumferential mean velocity component with radius will be considered in the form

$$U_s(r) = \Omega r + \Gamma / r \tag{7}$$

From the mean swirl profile (7) and relation (4), the following expression for the axial velocity component U_x is readily deduced:

$$U_x^2(r) - U_0^2 = -2[\Omega^2(r^2 - 1) + 2\Omega\Gamma \ell n(r)] \tag{8}$$

where U_0 is the axial velocity estimated at the mean radius of the duct. It will be shown in the numerical examples given later in this paper that this variation of the axial velocity component associated with the mean vortical swirl can be significant, and in some cases even higher than the corresponding variation of the swirling component.

For convenience, we specify the mean-flow parameters in terms of the Mach numbers of the axial and swirl mean velocity components $M_x = U_x/\bar{c}_0$ ($\bar{M}_x = U_0/\bar{c}_0$), $M_\Gamma = \Gamma/r\bar{c}_0$ ($\bar{M}_\Gamma = \Gamma/r_m\bar{c}_0$), and $M_\Omega = \Omega r/\bar{c}_0$ ($\bar{M}_\Omega = \Omega r_m/\bar{c}_0$), where $\bar{c}_0$ is the stagnation speed of sound.

Governing Equations for Unsteady Flow

The present linearized analysis of small-amplitude unsteady disturbances imposed on a swirling mean flow accounts for the distortion of the disturbances by the nonuniform mean flow but neglects the nonlinear inertial and viscous effects. With these assumptions the equations governing the perturbation velocity $\boldsymbol{u}$ and pressure p' are the linearized Euler equations

$$\frac{\mathrm{D}_0 \boldsymbol{u}}{\mathrm{D}t} + (\boldsymbol{u} \cdot \nabla)\boldsymbol{U} = -\nabla\left(\frac{p'}{\rho_0}\right) \tag{9}$$

$$\frac{\mathrm{D}_0}{\mathrm{D}t}\left(\frac{p'}{c_2^0 \rho_0}\right) + \frac{1}{\rho_0}\nabla \cdot \rho_0 \boldsymbol{u} = 0 \tag{10}$$

where $\mathrm{D}_0/\mathrm{D}t = \partial/\partial t + \boldsymbol{U} \cdot \nabla$ is the convective derivative and ρ_0 and c_0 are the mean-flow density and speed of sound, respectively. Both depend only on the radius r.

As mentioned earlier, the mean swirl couples the various disturbances, and therefore it is not possible, in general, to split the disturbances into separate entropic, potential, and vortical parts. However, it is always useful to examine the coupling between pressure-dominated and vorticity-dominated modes. To this end, we write

$$\boldsymbol{u} = \boldsymbol{u}^{(R)} + \nabla\phi \tag{11}$$

which reduces the equations of motion (9) and (10) to the following system of coupled equations:

$$\mathcal{L}_c \boldsymbol{u}^{(R)} = -\zeta_0 \times \nabla\phi \tag{12}$$

$$\mathcal{L}_w \phi = (1/\rho_0)\nabla \cdot \left[\rho_0 \boldsymbol{u}^{(R)}\right] \tag{13}$$

where ζ_0 is the mean-flow vorticity and $\mathcal{L}_c$ and $\mathcal{L}_w$ are, respectively, the operators of convection and wave propagation

$$\mathcal{L}_c \boldsymbol{u}^{(R)} \equiv \frac{\mathrm{D}_0 \boldsymbol{u}^{(R)}}{\mathrm{D}t} + \left[\boldsymbol{u}^{(R)} \cdot \nabla\right]\boldsymbol{U} \tag{14}$$

$$\mathcal{L}_w \phi \equiv \frac{\mathrm{D}_0}{\mathrm{D}t}\frac{1}{c_0^2}\frac{\mathrm{D}_0}{\mathrm{D}t}\phi - \frac{1}{\rho_0}\nabla \cdot (\rho_0 \nabla)\phi \tag{15}$$

The unsteady pressure field is now obtained solely in terms of the potential function

$$p' = -\rho_0 \frac{\mathrm{D}_0 \phi}{\mathrm{D}t} \tag{16}$$

Equations (12) and (13) describe the behavior of coupled pressure and vorticity modes of unsteady motions imposed on any isentropic nonuniform vortical mean flow. For confined flows an additional coupling is produced at the walls.

Equation (13) indicates that, because of the nonuniformity of the mean flow, an inlet vortical perturbation will induce an unsteady hydrodynamic pressure field. Moreover, in contrast to a classical vortical gust that preserves its initial form as it convects uniformly, a swirling mean flow can induce centrifugal and Coriolis forces that create a force imbalance and deflect the motion of fluid particles. For a potential mean swirl there are only centrifugal forces, and, as will be shown, the vortical disturbance will grow algebraically as it travels downstream. For a vortical mean swirl ($\Omega \neq 0$) Eq. (12) shows additional local Coriolis forces that can either restore the force balance creating wave oscillations or lead to exponential growth. This interaction thus introduces a length scale to characterize either the oscillations, or the rate of growth of the instability.

Purely convected disturbances could only exist if there were a perfect balance between centrifugal and Coriolis forces. In practice, this balance is not realized, and therefore a critical layer appears in the eigenvalue spectrum corresponding to the purely convected modes.

To estimate the relative effect of the mean swirl on the behavior of vortical and acoustic perturbations of the flow, we consider the Rossby number $\bar{\omega} r / U_s$, where $\bar{\omega}$ is the frequency of the unsteady disturbance in a frame of reference moving with the local mean-flow velocity. For potential (acoustic-like) disturbances the Rossby number is typically large and of the order of the number of the cascade blades.[2] Thus, one would expect that the effect of swirl will be mostly limited to the Doppler shift of the cut-on frequencies for propagating pressure-dominated modes and to the refraction of these modes by the nonuniform flow. The accurate analysis and determination of these modes is, however, essential for the correct formulation of outflow radiation conditions.[8]

On the other hand, nearly convected vortical disturbances will evolve with a timescale of the order of r/U_s, i.e., the Rossby number for them is of order unity. Therefore, the centrifugal and Coriolis forces will have a strong effect on these modes as shown from the asymptotic normal mode analysis in Ref. 4. This analysis further indicates that for a potential free vortex swirl there is a continuum spectrum of convected eigenvalues, whereas for a vortical swirl two branches of discrete nearly convected neutral eigenvalues can appear on either sides of the critical layer and accumulate at its boundaries.

Gust in a Swirling Flow

We now focus our attention on the representation of the upstream disturbances. The normal mode analysis in Refs. 3 and 4 shows that the corresponding boundary-value problem is not self-adjoint. As a result, the eigenmodes are not orthogonal and may not form a complete set. Moreover, in a vortical swirling flow the eigenvalues accumulate with increasing density near the edges of a critical layer. Therefore, it is not practical to use the corresponding nearly convected eigenmodes to represent the upstream disturbances. In the special case of a mean flow with pure solid-body rotation, Howe and Liu[9] obtained an analytical expression for the nearly convected modes to represent an incident axisymmetric vorticity wave. For the more general case Montgomery and Verdon[10] assumed, for simplicity, a purely convected vortical disturbance. Such approaches do not represent all possible upstream disturbances, and in particular they neglect spatially developing solutions. Moreover, the normal mode analysis cannot represent those spatially developing solutions that may be convectively unstable for certain mean-flow configurations.

We therefore propose to describe the upstream disturbances using the eigenmode representation for the nearly sonic, pressure-dominated modes and an initial-value analysis to represent the nearly convected, vorticity-dominated modes. We further assume that the unsteady pressure and velocity data are given at a cross section defined by $x = 0$.

We begin by splitting the flow quantities as

$$\phi = \phi_{(s)} + \phi_{(c)}, \qquad p' = p'_{(s)} + p'_{(c)}, \qquad \boldsymbol{u}^{(R)} = \boldsymbol{u}^{(R)}_{(s)} + \boldsymbol{u}^{(R)}_{(c)} \tag{17}$$

where the subscript (s) denotes the nearly sonic modes and (c) denotes the nearly convected modes (purely convected in a potential mean flow). The unsteady pressure associated with the pressure-dominated (s) modes is then expanded as

$$p'_{(s)}(x, r, \theta, t) = \int_\omega \sum_m \sum_n b_{mn} P_{(s)mn}(r) \times \exp[i(k_{mm} x + m\theta - \omega t)]\, \mathrm{d}\omega \tag{18}$$

where $P_{(s)mn}$ represent the pressure-dominated eigenmodes and k_{mn} the corresponding eigenvalues. Similar expressions can also be written for $\phi_{(s)}$ and $\boldsymbol{u}^{(R)}_{(s)}$, with $\phi_{(s)mn}$, $X_{(s)mn}$, $R_{(s)mn}$, and $T_{(s)mn}$ instead of $P_{(s)mn}$ for the potential function and the axial, radial, and circumferential vortical velocities, respectively. Note that $\phi_{(s)mn}$, $X_{(s)mn}$, $R_{(s)mn}$, and $T_{(s)mn}$ can be expressed in terms of $P_{(s)mn}$ (Ref. 4). We also require that this nearly sonic velocity field satisfy the impermeability condition along the walls, i.e., $R_{(s)mn} + \mathrm{d}\phi_{(s)mn}/\mathrm{d}r = 0$ at $r = r_h$ and r_t, where r_h and r_t represent the radii at the hub and tip, respectively.

For the vorticity-dominated (c) modes we start the initial-value analysis by assuming the following expansion for the vortical velocity:

$$\boldsymbol{u}^{(R)}_{(c)}(x, r, \theta, t) = \int_\omega \sum_m \boldsymbol{A}_m(x, r) \exp[i(\alpha_r x + m\theta - \omega t)]\, \mathrm{d}\omega \tag{19}$$

where $\boldsymbol{A}_m(x, r)$ is to be determined numerically in terms of the inlet disturbance and α_r is given by the condition

$$\frac{\mathrm{D}_0}{\mathrm{D}t}(\alpha_r x + m\theta - \omega t) = 0 \tag{20}$$

This defines

$$\alpha_r = (\omega - m U_s / r)/U_x \tag{21}$$

In what follows, we consider only a single (ω, m) Fourier component of the disturbance pressure and velocity

$$p'^{(m)}(x, r, \theta, t) = p'(x, r) e^{i(m\theta - \omega t)}$$
$$\boldsymbol{u}^{(m)}(x, r, \theta, t) = \boldsymbol{u}(x, r) e^{i(m\theta - \omega t)} \tag{22}$$

and similarly for separate vortical and potential velocity components.

The vortical velocity $\boldsymbol{u}^{(R)}_{(c)}$ and the associated potential $\phi_{(c)}$ [see Eq. (13)] define the generalized gust velocity. An initial-value analysis of Eqs. (12) and (13) will, in general, require upstream and downstream conditions for $\phi_{(c)}$ and an upstream condition for $\boldsymbol{u}^{(R)}_{(c)}$. We now recall that the results of the eigenmode analysis[4] have shown that the unsteady pressure associated with the (c) modes is rather small. We therefore identify all of the upstream pressure with the pressure-dominated (s) modes $P_{(s)mn}$, i.e.,

$$p'(0, r) \sim p'_{(s)}(0, r) = \sum_n b_{mn} P_{(s)mn}(r) \tag{23}$$

Hence, unless specific information is provided about the nearly convected pressure field, we assume the following initial condition at $x = 0$ for $\phi^{(m)}_{(c)}$:

$$\frac{\mathrm{D}_0}{\mathrm{D}t} \phi^{(m)}_{(c)} = 0 \tag{24}$$

and a homogeneous downstream condition for $\phi^{(m)}_{(c)}$, which will be discussed later.

The imposed upstream perturbation velocity at $x = 0$ can now be expressed as

$$\boldsymbol{u}(0, r) = \boldsymbol{u}_{(s)}(0, r) + \boldsymbol{u}_{(c)}(0, r) \tag{25}$$

where $\boldsymbol{u}_{(s)}(0, r)$ corresponds to $p'_{(s)}(0, r)$ and whose expression is determined from Eq. (23). The nearly convected velocity is

$$\boldsymbol{u}_{(c)}(x, r) = \boldsymbol{A}_m(x, r) e^{i\alpha_r x} + e^{-im\theta} \nabla\left[\phi_{(c)}(x, r) e^{im\theta}\right] \tag{26}$$

where $\boldsymbol{A}_m$ and $\phi_{(c)}$ are solution to Eqs. (12) and (13). For a given $\boldsymbol{A}_m(0, r)$ and homogeneous boundary conditions for $\phi_{(c)}$, the potential function $\phi_{(c)}$ can be fully determined in terms of $\boldsymbol{A}_m(x, r)$.

It is convenient to expand $\boldsymbol{A}_m(0, r)$ in terms of known basis functions satisfying impermeability at the wall and reproducing the classical limit for a vortical gust in a uniform flow. This will facilitate comparison with the linear cascade results. To this end, we assume the following expansion for the radial, circumferential, and axial components of $\boldsymbol{A}_m(0, r)$:

$$A_{rm}(0, r) = \sum_n A_{rmn} K_1(\mu_n r)$$

$$A_{\theta m}(0, r) = \left(A_{\theta m0} + \sum_n A_{\theta mn} K_2(\mu_n r)\right) r$$

$$A_{xm}(0, r) = A_{xm0} + \sum_n [A_{xmn} K_2(\mu_n r) + B_{xmn} K_3(\mu_n r)] \quad (27)$$

where A_{rmn}, $A_{\theta mn}$, A_{xmn}, B_{xmn} are constants and μ_n are determined from the wall condition $K_1(\mu_n r_h) = K_1(\mu_n r_t) = 0$, for $n = 1, 2, \ldots$. The functions $K_1(\mu_n r)$, $K_2(\mu_n r)$, and $K_3(\mu_n r)$ form an orthogonal set and are defined in terms of Hankel functions:

$$K_1(\mu_n r) = i D_1 \sqrt{r}\left[H_1^{(1)}(\mu_n r) + \kappa H_1^{(2)}(\mu_n r)\right]$$

$$K_2(\mu_n r) = i D_0 \sqrt{r}\left[H_0^{(1)}(\mu_n r) + \kappa H_0^{(2)}(\mu_n r)\right]$$

$$K_3(\mu_n r) = D_0 \sqrt{r}\left[H_0^{(1)}(\mu_n r) - \kappa H_0^{(2)}(\mu_n r)\right]$$

with constants

$$D_1 = -\pi \sqrt{r_h} H_1^{(2)}(\mu_n r_h)/4, \qquad D_0 = -\pi \sqrt{r_h} H_0^{(2)}(\mu_n r_h)/4$$

$$\kappa = -H_1^{(1)}(\mu_n r_h)/H_1^{(2)}(\mu_n r_h)$$

In the two-dimensional limit of $b/r_h \ll 1$ ($b = r_t - r_h$), these functions reduce to the conventional form of a gust in the linear cascade model

$$K_1(\mu_n r), K_3(\mu_n r) \sim \sin(\pi n/b)(r - r_h)$$

$$K_2(\mu_n r) \sim \cos(\pi n/b)(r - r_h)$$

Finally, when comparing the present results with those of a gust in a uniform flow, we impose the condition at $x = 0$:

$$(i\omega/U_0) A_{xmn} + \mu_n A_{rmn} + im A_{\theta mn} = 0 \quad (28)$$

which corresponds to the divergence-free condition that must be satisfied by a vortical disturbance in a uniform flow.

Potential Swirl

When the mean swirl is potential ($\Omega = 0$), the mean velocity is represented by

$$\boldsymbol{U}(\boldsymbol{x}) = U_x \hat{e}_x + (\Gamma/r)\hat{e}_\theta \quad (29)$$

where $U_x = U_0 = \text{const}$ for a uniform stagnation enthalpy across the annulus. The forcing Coriolis term in Eq. (12) drops out and $\boldsymbol{u}_{(s)}^{(R)} = 0$. The vortical velocity $\boldsymbol{u}_{(c)}^{(R)}$ is uncoupled from the pressure and satisfies the homogeneous equation

$$\mathcal{L}_c \boldsymbol{u}_{(c)}^{(R)} = 0 \quad (30)$$

Substituting Eq. (19) into Eq. (30) and integrating for $t > 0$ and $x > 0$ gives the amplitude vector $\boldsymbol{A}_m(x, r)$ in the form

$$\boldsymbol{A}_m(x, r) = \boldsymbol{a}(r) + x\boldsymbol{b}(r) \quad (31)$$

where the vectors $\boldsymbol{a}(r)$ and $\boldsymbol{b}(r)$ are expressed in terms of the initial gust conditions:

$$\boldsymbol{a}(r) = [A_{xm}(0, r), A_{rm}(0, r), A_{\theta m}(0, r)]$$

$$\boldsymbol{b}(r) = \left[0, \left(2\Gamma / U_0 r^2\right) A_{\theta m}(0, r), 0\right] \quad (32)$$

This solution shows that, as a result of unbalanced centrifugal forces, the radial component of the vortical velocity will grow linearly as the vortical waves are convected downstream.

The potential $\phi_{(c)}$ associated with $\boldsymbol{u}_{(c)}^{(R)}$ is obtained numerically as a particular solution to the nonhomogeneous wave equation (13) and determines the hydrodynamic pressure associated with the gust. Introducing the transformation

$$\phi_{(c)}(x, r, \theta, t) = \psi_{(c)}(x, r) \exp[i(\alpha_r x + m\theta - \omega t)] \quad (33)$$

and taking into account the vortical solution [Eqs. (31) and (32)], the boundary-value problem for Eq. (13) is reduced to two variables (x, r), with the wall impermeability condition

$$\frac{\partial \phi_{(c)}}{\partial r} + u_{r(c)}^{(R)} = 0 \quad (34)$$

Furthermore, considering the far downstream expansion of Eq. (13), it can be easily shown that for nonaxisymmetric disturbances

$$\psi_{(c)}(x \to \infty, r) = (ir/m) A_{\theta m}(0, r) + \mathcal{O}(1/x) \qquad m \neq 0 \quad (35)$$

Thus the radial component of the potential velocity associated with the gust has the asymptotic behavior

$$\frac{\partial \phi_{(c)}}{\partial r}(x \to \infty, r, \theta, t) = -\frac{2\Gamma x}{U_0 r^2} A_{\theta m}(0, r) \times \exp[i(\alpha_r x + m\theta - \omega t)] + \mathcal{O}(1), \qquad m \neq 0 \quad (36)$$

This completely cancels the linear growth of the vortical radial component of the velocity. Thus, the total generalized gust velocity will remain finite, whereas its vorticity will grow linearly (because of the stretching) as the gust propagates downstream.

The unsteady pressure associated with the incident gust is given by

$$p'_{(c)}(x, r, \theta, t) = -\rho_0 U_0 \frac{\partial \psi_{(c)}}{\partial x} \exp[i(\alpha_r x + m\theta - \omega t)] \quad (37)$$

The asymptotic solution (35) indicates a slow (algebraic) decay of the gust nonaxisymmetric pressure perturbations far downstream, as a result of phase cancellations. This conclusion is also consistent with analyses by Tan and Greitzer[11] and Wundrow.[12]

For axisymmetric disturbances $m = 0$ ($\alpha_r = \omega/U_0$), Eq. (31) suggests the following expansion form for $\psi_{(c)}(x, r)$ as $x \to \infty$:

$$\psi_{(c)}(x, r) = \sigma_1(r) + x\sigma_2(r) \quad (38)$$

where the radial functions $\sigma_1(r)$ and $\sigma_2(r)$ satisfy nonhomogeneous ordinary differential equations of the Bessel type. It follows immediately from Eq. (37) that the hydrodynamic pressure does not decay but rather remains finite far downstream in the duct.

The numerical solution for $\psi_{(c)}(x, r)$ is, in general, obtained using a second-order accurate finite difference scheme. To illustrate the results, we examine the downstream evolution of the gust with imposed (at $x = 0$) perturbation $A_{\theta mn} = 1$, $A_{xmn} = 0$, and A_{rmn} determined from Eq. (28) in an annular duct $0.8 \le r \le 1.2$. A free-vortex mean swirling flow with $\bar{M}_\Gamma = 0.3$ is superimposed on a uniform axial mean flow with $\bar{M}_x = 0.3$ (Fig. 2). The unsteady gust with modal numbers $m = 2$ and $n = 1$ is excited with frequency $\bar{\omega} = \omega r_m/\bar{c}_0 = 8$. Figure 3 shows the evolution of the axial and circumferential disturbance velocity components (which determine the blade upwash for the gust response problem) and the induced hydrodynamic pressure along the mean-flow streamline $\theta = x\Gamma/U_0 r^2$ at $r = 0.9$. According to relations (33) and (35), the gust velocity components asymptotically tend as $x \to \infty$ to $u_{x(c)} \to -\alpha_r r A_{\theta m}(0, r)/m \approx 7.5$ and $u_{\theta(c)} \to 0$. The magnitude of the induced convected pressure remains relatively small and tends to zero. The transition occurs slowly, over a large axial distance.

In practical applications related to the blade-response problem, one would be interested in the gust evolution over a distance of the order of interstage axial spacing. Figure 4 illustrates the change of

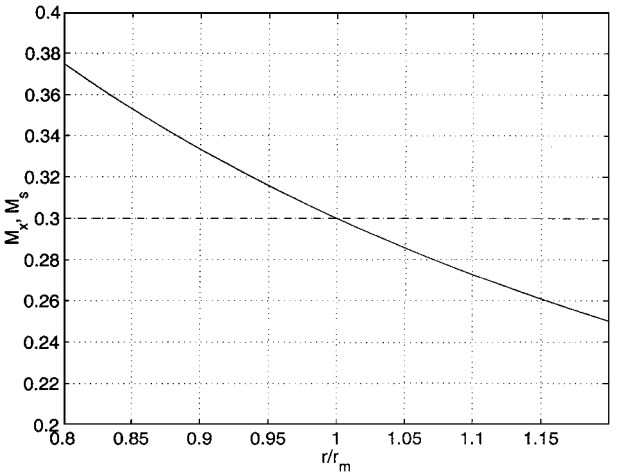

Fig. 2 Radial variation of $M_s(r)$ (——) and $M_x(r)$ (– – –) for $\bar{M}_x = 0.3$, and $\bar{M}_\Gamma = 0.3$.

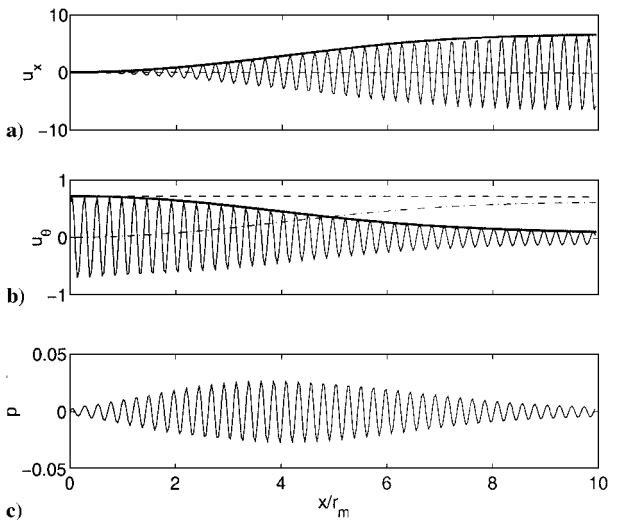

Fig. 3 Evolution of the a) gust axial and b) circumferential velocity components and c) pressure for $\bar{M}_x = 0.3$, $\bar{M}_\Gamma = 0.3$, $\bar{\omega} = 8$, $A_{\theta mn} = 1$, $m = 2$, $n = 1$, and $r = 0.9$: ——, magnitude and real values; – – –, magnitude of vortical velocity component; and – ·–, magnitude of potential velocity component.

the radial profile of the imposed gust velocity as a result of the gust evolution from $x = 0$ to 1. The axial component, which is initially small, becomes significant as its potential part grows, while the circumferential component remains practically unchanged.

Vortical Swirl

For a vortical swirl we consider the following mean velocity field

$$\boldsymbol{U}(\boldsymbol{x}) = U_x(r)\hat{e}_x + (\Omega r + \Gamma/r)\hat{e}_\theta \tag{39}$$

where $U_x(r)$ is determined by Eq. (8) and the mean vorticity ζ_0 has both axial and circumferential components

$$\zeta_0 = 2\Omega\hat{e}_x - \frac{\mathrm{d}U_x}{\mathrm{d}r}\hat{e}_\theta \tag{40}$$

where $\mathrm{d}U_x/\mathrm{d}r = -2\Omega(\Omega r + \Gamma/r)/U_x$. Substituting Eq. (39) into Eq. (12), we obtain

$$\frac{\mathrm{D}_0 u^{(R)}_{x(c)}}{\mathrm{D}t} + u^{(R)}_{r(c)}\frac{\mathrm{d}U_x}{\mathrm{d}r} = -\frac{\mathrm{d}U_x}{\mathrm{d}r}\frac{\partial\phi_{(c)}}{\partial r} \tag{41}$$

$$\frac{\mathrm{D}_0 u^{(R)}_{r(c)}}{\mathrm{D}t} - 2\left(\Omega + \frac{\Gamma}{r^2}\right)u^{(R)}_{\theta(c)} = \frac{2\Omega}{r}\frac{\partial\phi_{(c)}}{\partial\theta} + \frac{\mathrm{d}U_x}{\mathrm{d}r}\frac{\partial\phi_{(c)}}{\partial x} \tag{42}$$

$$\frac{\mathrm{D}_0 u^{(R)}_{\theta(c)}}{\mathrm{D}t} + 2\Omega u^{(R)}_{r(c)} = -2\Omega\frac{\partial\phi_{(c)}}{\partial r} \tag{43}$$

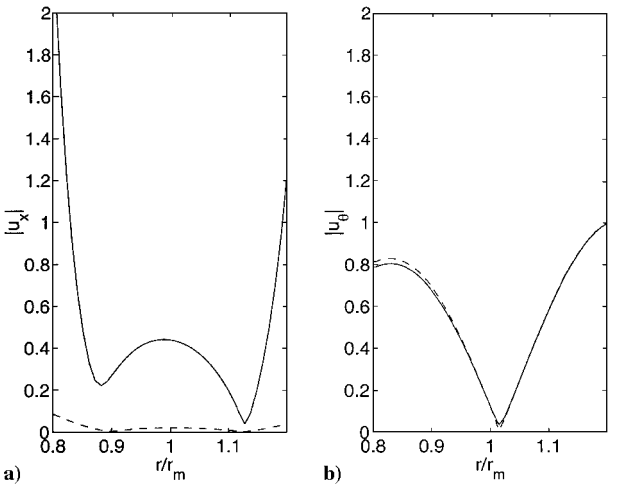

Fig. 4 Evolution of the a) gust axial and b) circumferential velocity profiles from $x = 0$ (– – –) to 1 (——) for $\bar{M}_x = 0.3$, $\bar{M}_\Gamma = 0.3$, $\bar{\omega} = 8$, $A_{\theta mn} = 1$, $m = 2$, and $n = 1$.

Comparing Eqs. (41) and (43), one can see that the axial and circumferential vortical velocities are related by

$$u^{(R)}_{x(c)} = u^{(R)}_{x(c)0} + \frac{\mathrm{d}U_x/\mathrm{d}r}{2\Omega}u^{(R)}_{\theta(c)} \tag{44}$$

where $u^{(R)}_{x(c)0}$ is a purely convected quantity. Thus, to solve the initial-value problem, it is enough to consider a coupled system of Eqs. (13), (42), and (43).

If we formally neglect the variation of the axial mean velocity component, hence discarding condition (4) of uniform stagnation enthalpy, then the axial component $u^{(R)}_{x(c)}$ becomes completely uncoupled and is then convected independently of the other gust components. For simplicity, such an assumption has been adopted in previous approaches to the problem (e.g., Ref. 2). However, it is important to calculate accurately $u^{(R)}_{x(c)}$ because it contributes significantly to the unsteady upwash along the downstream blading.

It is convenient to decompose the solutions of Eqs. (13) and (41–43) into a homogeneous solution $\{\boldsymbol{u}^{(R)}, \phi\}_{(c)h}$, accounting for the upstream disturbance condition, and a particular solution $\{\boldsymbol{u}^{(R)}, \phi\}_{(c)p}$ with homogeneous upstream conditions. For $t > 0$ and $x \geq 0$, $\boldsymbol{u}^{(R)}_{(c)h}$ can be determined for every m component $\boldsymbol{A}_{hm}(x, r)$ in terms of the initial gust conditions (27) at $x = 0$:

$$\begin{aligned}
A_{rhm}(x, r) &= A_{rm}(0, r)\cos(\lambda/U_x)x \\
&\quad + A_{\theta m}(0, r)(\lambda/2\Omega)\sin(\lambda/U_x)x \\
A_{\theta hm}(x, r) &= A_{\theta m}(0, r)\cos(\lambda/U_x)x \\
&\quad - A_{rm}(0, r)(2\Omega/\lambda)\sin(\lambda/U_x)x \\
A_{xhm}(x, r) &= A_{xm}(0, r) + (U_s/U_x)[A_{\theta m}(0, r) - A_{\theta hm}(x, r)]
\end{aligned} \tag{45}$$

where

$$\lambda(r) = 2\sqrt{\Omega(\Omega + \Gamma/r^2)} \tag{46}$$

Solutions (45) reduce to Eqs. (31) and (32) in the limit of $\Omega \to 0$.

This result clearly shows that the Coriolis forces create an interactive oscillatory exchange mechanism between the various components of the vortical velocity, and thus introduce an additional characteristic wave number for the nearly convected disturbances λ/U_x. This wave number may vary significantly for modes propagating at different radii of the duct.

The parameter λ in Eq. (46) becomes purely imaginary if $\Omega(\Omega + \Gamma/r^2) < 0$, which is similar to Rayleigh criterion for centrifugal instability in the flow. In this case the homogeneous solutions (45) amplify or decay exponentially, and so does the total generalized gust solution.

The potential gust response $\phi_{(c)h}$ is obtained as a particular solution to the convective wave equation

$$\mathcal{L}_w \phi_{(c)h} = (1/\rho_0)\nabla \cdot \left[\rho_0 \boldsymbol{u}^{(R)}_{(c)h}\right] \tag{47}$$

As for the case of a potential swirl, a solution is sought in the form

$$\phi_{(c)h} = \psi_{(c)h}(x, r)\exp[i(\alpha_r x + m\theta - \omega t)] \tag{48}$$

which reduces Eq. (47) to an elliptic equation for the nearly convected potential perturbations. This boundary-value problem is solved with the wall impermeability condition, which provides an additional coupling between the vortical and potential components $\partial\phi_{(c)h}/\partial r + u^{(R)}_{r(c)h} = 0$ at $r = r_h$ and $r = r_t$. Upstream at $x = 0$, we assume [consistent with Eq. (24)] a pressure-less gust condition, $p'_{(c)h}(0, r) = 0$. Equations (45) suggest that $\psi_{(c)h}(x, r)$ acts as a wave envelope whose behavior is dominated by the Coriolis oscillations with wave number λ/U_x. Numerical experiments also confirmed this dominant behavior. We therefore propose the following outflow boundary condition:

$$\frac{\partial^2 \psi_{(c)h}}{\partial x^2} + \frac{\lambda^2}{U_x^2}\psi_{(c)h} = 0 \tag{49}$$

Finally, we need to determine the particular part of the generalized gust solution $\{\boldsymbol{u}^{(R)}, \phi\}_{(c)p}$, which results from the mutual potential-vortical coupling in Eqs. (12) and (13). By construction, this particular solution is produced by $\phi_{(c)h}$ and governed by the coupled system of equations

$$\mathcal{L}_c \boldsymbol{u}^{(R)}_{(c)p} = -\zeta_0 \times \nabla\left[\phi_{(c)h} + \phi_{(c)p}\right] \tag{50}$$

$$\mathcal{L}_w \phi_{(c)p} = (1/\rho_0)\nabla \cdot \left[\rho_0 \boldsymbol{u}^{(R)}_{(c)p}\right] \tag{51}$$

It is therefore possible to assume

$$\phi_{(c)p} = \psi_{(c)p}(x, r)\exp[i(\alpha_r x + m\theta - \omega t)] \tag{52}$$

Equations (50) and (51) are solved numerically for the amplitude vector $\boldsymbol{A}_{pm}(x, r) = \{A_{xpm}, A_{rpm}, A_{\theta pm}\}$ of the vortical velocity and the coupled potential amplitude $\psi_{(c)p}(x, r)$. The numerical procedure solves Eqs. (50) and (51) iteratively by taking for the first iteration $\boldsymbol{A}_{pm}(0, r) = 0$ and the pressureless condition $\partial\psi_{(c)p}(0, r)/\partial x = 0$. The impermeability condition $\partial\phi_{(c)p}/\partial r = -A_{rpm}$ is applied at the duct walls and the condition (49) for $\psi_{(c)p}$ at the outflow boundary.

The downstream evolution of unsteady vortical disturbances imposed on a vortical swirling mean flow is now illustrated for two cases of stable [real $\lambda(r)$] and unstable [imaginary $\lambda(r)$] flows. In the first case the radial variation of the mean flow is determined by specifying the following mean-radius Mach numbers of the mean velocity components $\bar{M}_x = 0.3$, $\bar{M}_\Gamma = 0.1$, and $\bar{M}_\Omega = 0.2$. Such a swirl produces a very significant variation of the mean axial velocity component with radius (in Fig. 5). In the second case the mean flow is specified by taking $\bar{M}_x = 0.3$, $\bar{M}_\Gamma = 0.2$, and $\bar{M}_\Omega = -0.2$. The resulting mean flow (in Fig. 6) leads to unstable flow conditions for $r < 1$ and to stable flow conditions for $r > 1$.

As for the case of a potential swirl, a vortical perturbation with $A_{\theta mn} = 1$, $A_{xmn} = 0$, and A_{rmn} from Eq. (28) is imposed at $x = 0$ in a duct $0.8 \le r \le 1.2$, with $\bar{\omega} = 8$, $m = 2$, and $n = 1$. The results are shown for the gust velocity and pressure downstream evolution along the mean-flow streamline $\theta = x(\Omega + \Gamma/r^2)/U_x$ at the radius $r = 0.9$. For the stable flow (Fig. 7) the results clearly indicate a superposition of two characteristic wave numbers ω/U_x and λ/U_x, with the latter acting as an envelope for the high-frequency oscillations of the former. This particular solution reduces the effects of the modulation by the envelope as the disturbances propagate downstream. This results from accounting for all of the eigenmodes behavior including the critical layer. To illustrate this effect, Fig. 8 compares the present results (solid line) for $|u_{\theta(c)}|$ with those using the eigenmode approaches of Ref. 10 (dashed-dotted line) and Ref. 9 (dashed line). The latter is obtained from superposition of two eigenmodes corresponding to the extreme points of the nearly convected spectrum. The modification of the gust axial and circumferential velocity components over the distance $\Delta x = 1$ is shown in

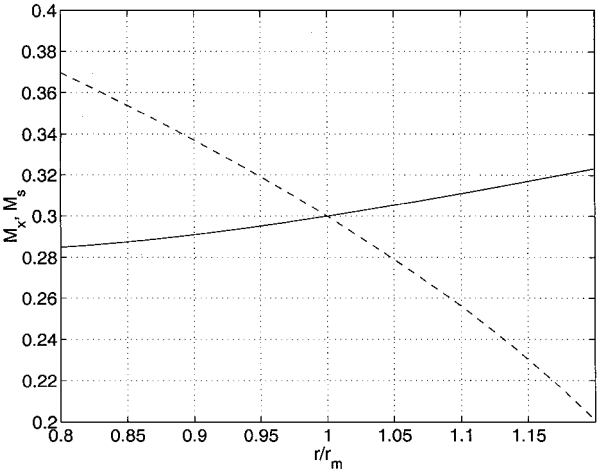

Fig. 5 Radial variation of $M_s(r)$ (——) and $M_x(r)$ (– – –) for $\bar{M}_x = 0.3$, $\bar{M}_\Omega = 0.2$, and $\bar{M}_\Gamma = 0.1$.

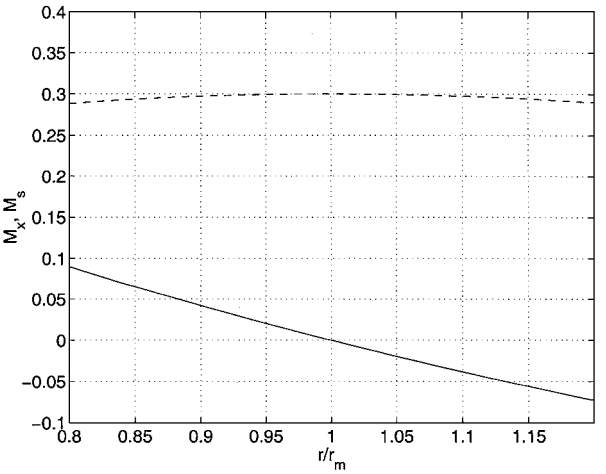

Fig. 6 Radial variation of $M_s(r)$ (——) and $M_x(r)$ (– – –) for $\bar{M}_x = 0.3$, $\bar{M}_\Omega = -0.2$, and $\bar{M}_\Gamma = 0.2$.

Figs. 9a and 9b, respectively. These results show a significant redistribution in the radial direction and imply strong three-dimensional effects of the mean swirl on the incident disturbances. This also underlines the importance of the initial-value approach for accurate predictions of the blade response.

In Fig. 10 we show the same unsteady perturbation propagating in the unstable region of the flow (at $r = 0.9$). The results reveal an amplification of all of the gust components. Far downstream the disturbance growth will violate the conditions of linearization, and hence nonlinear effects will become important. However, in most practical cases the growth of the instability scales with the radius of the annulus, which is typically of the order of the interstage gap between the fan rotor and stator, and thus justifies the present linear approach. For instance, in Fig. 11 the gust velocity profile at $x = 1$ remains of the same order of magnitude as the initial disturbance, although it has clearly undergone a notable modification, particularly at the unstable hub region.

In Figs. 12 and 13 we examine the ratio of the magnitudes of the perturbation velocity circumferential component of the gust $u_{\theta(c)}$ at $x = 1$ and 0, for the two cases of the mean swirl (stable, unstable) over a range of modal numbers m and n. For the stable case (Fig. 12) the effects are most significant for the first radial harmonic and for higher positive m. The increase in the amplitude ratio is more pronounced near the tip where the swirl component is dominant in the mean velocity profile. In contrast with the case of a stable flow, the unstable case results (Fig. 13) clearly show significant amplification for all values of the modal numbers at $r = 0.9$. For higher radial modes the growth rate remains practically at the same level for a broad range of m. On the other hand, at $r = 1.1$ (stable region) the

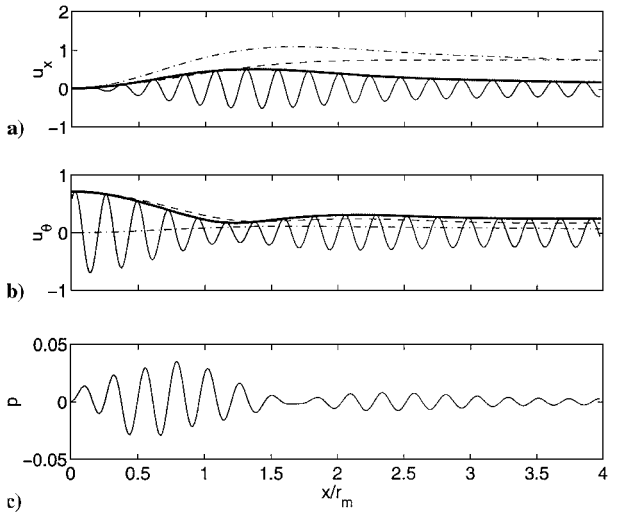

Fig. 7 Evolution of the a) gust axial and b) circumferential velocity components and c) pressure for $\bar{M}_x = 0.3$, $\bar{M}_\Omega = 0.2$, $\bar{M}_\Gamma = 0.1$, $\bar{\omega} = 8$, $A_{\theta mn} = 1$, $m = 2$, $n = 1$, and $r = 0.9$: ——, magnitude and real values; – – –, magnitude of vortical velocity component; and – ·–, magnitude of potential velocity component.

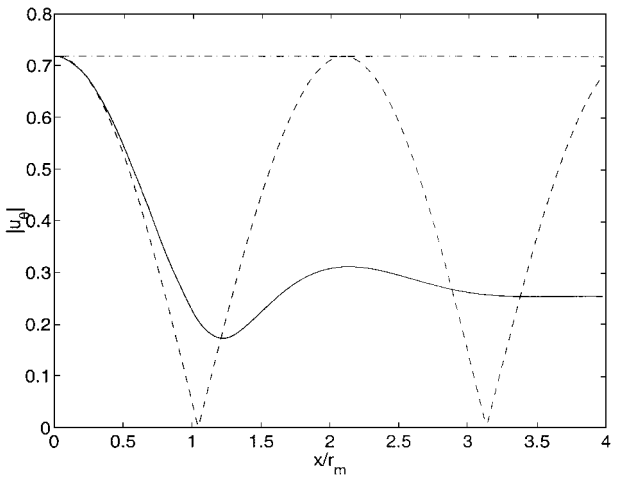

Fig. 8 Evolution of the gust circumferential velocity component $|u_{\theta(c)}|$ for $\bar{M}_x = 0.3$, $\bar{M}_\Omega = 0.2$, $\bar{M}_\Gamma = 0.1$, $\bar{\omega} = 8$, $A_{\theta mn} = 1$, $m = 2$, $n = 1$, and $r = 0.9$: ——, initial-value analysis; – – –, superposition of two nearly convected eigenmodes; and – ·–, convected eigenmode.

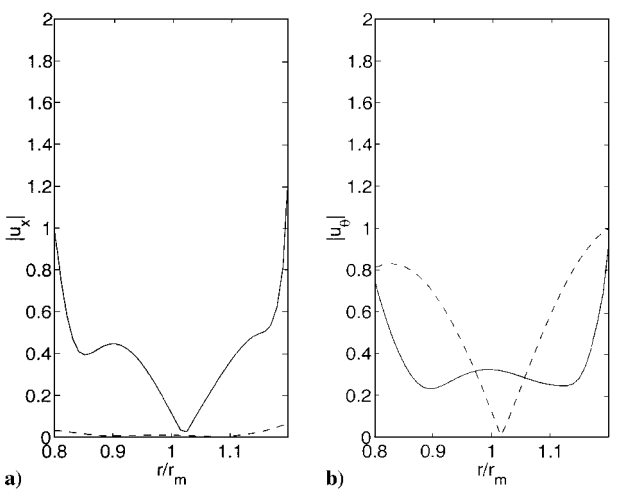

Fig. 9 Evolution of the a) gust axial and b) circumferential velocity profiles from $x = 0$ (– – –) to $x = 1$ (——) for $\bar{M}_x = 0.3$, $\bar{M}_\Omega = 0.2$, $\bar{M}_\Gamma = 0.1$, $\bar{\omega} = 8$, $A_{\theta mn} = 1$, $m = 2$, and $n = 1$.

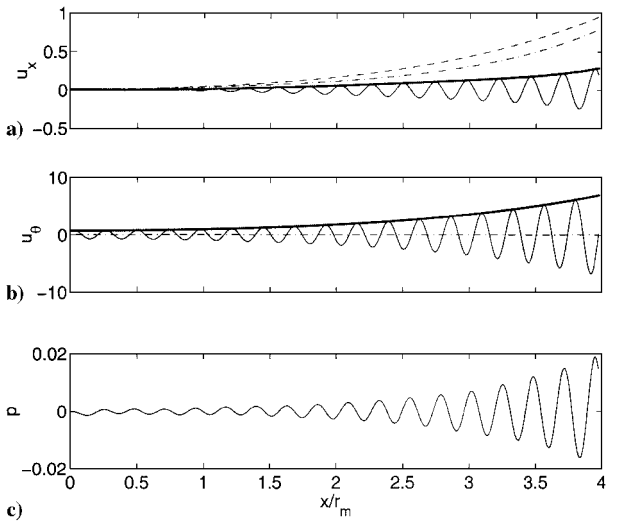

Fig. 10 Evolution of the a) gust axial and b) circumferential velocity components and c) pressure for $\bar{M}_x = 0.3$, $\bar{M}_\Omega = -0.2$, $\bar{M}_\Gamma = 0.2$, $\bar{\omega} = 8$, $A_{\theta mn} = 1$, $m = 2$, $n = 1$, and $r = 0.9$: ——, magnitude and real values; – – –, magnitude of vortical velocity component; and – ·–, magnitude of potential velocity component.

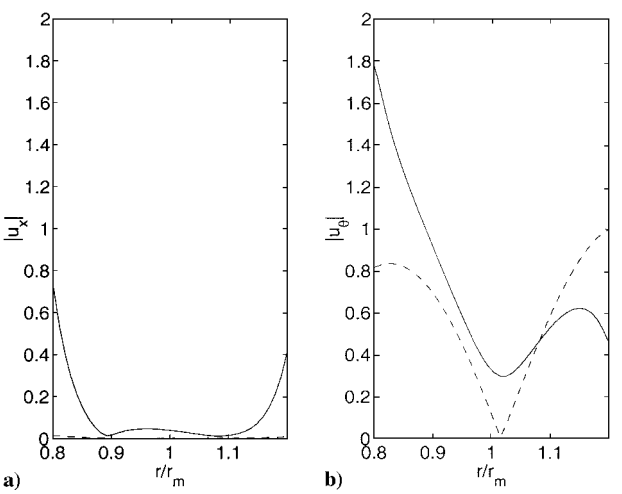

Fig. 11 Evolution of the a) gust axial and b) circumferential velocity profiles from $x = 0$ (– – –) to $x = 1$ (——) for $\bar{M}_x = 0.3$, $\bar{M}_\Omega = -0.2$, $\bar{M}_\Gamma = 0.2$, $\bar{\omega} = 8$, $A_{\theta mn} = 1$, $m = 2$, and $n = 1$.

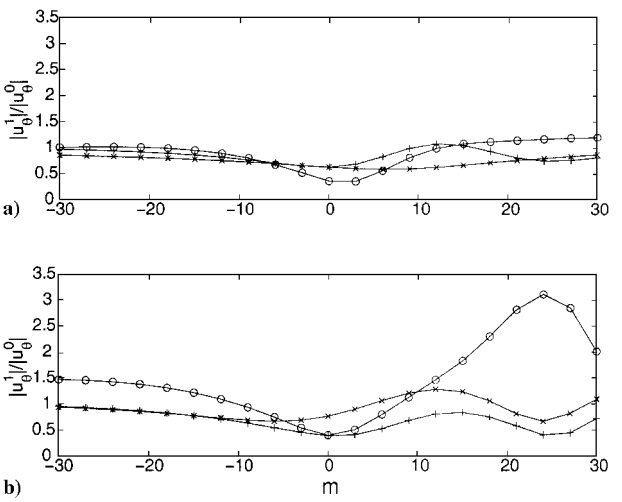

Fig. 12 Ratio of the circumferential gust velocity magnitudes at $x = 1$ and 0 for a) $r = 0.9$ and b) $r = 1.1$: ∘, $n = 1$; +, $n = 3$; ×, $n = 5$. $\bar{M}_x = 0.3$, $\bar{M}_\Omega = 0.2$, $\bar{M}_\Gamma = 0.1$, $\bar{\omega} = 8$, and $A_{\theta mn} = 1$.

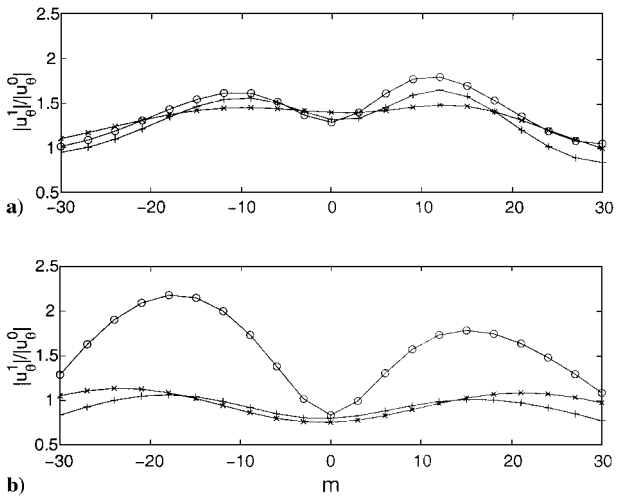

Fig. 13 Ratio of the circumferential gust velocity magnitudes at $x = 1$ and 0 for a) $r = 0.9$ and b) $r = 1.1$: ○, $n = 1$; +, $n = 3$; ×, $n = 5$. $\bar{M}_x = 0.3$, $\bar{M}_\Omega = -0.2$, $\bar{M}_\Gamma = 0.2$, $\bar{\omega} = 8$, and $A_{\theta mn} = 1$.

most significant change in the magnitude ratio occurs for the first radial mode and for the highly nonaxisymmetric flow perturbations. The higher radial modes show a decay of $|u_{\theta(c)}|$ for most of the considered range of m. The results in both regions indicate a practically symmetric behavior of amplitudes for the nearly convected modes spinning in the direction and opposite to the direction of the mean swirl. This effect, however, can depend on the choice of the parameters.

The analysis presented in Part 1 enables us to calculate the blade unsteady upwash and thus paves the way for the treatment of the blade aerodynamic response problem presented in Part 2 (Ref. 13).

Conclusions

An analysis of the interaction of unsteady swirling flows with annular cascades is presented in two parts. In Part 1 we focused on the description and evolution of incident disturbances in a mean swirling flow. An eigenmode analysis has shown that the centrifugal and Coriolis forces couple the acoustic and vortical modes and lead to the formation of a critical layer in the convected spectrum. Moreover, for moderate subsonic Mach numbers the eigenmodes can be segregated into pressure-dominated and vorticity-dominated modes. To describe completely the incident disturbances and avoid the difficulties associated with the critical layer, we represent the incident disturbances in terms of the pressure-dominated eigenmodes and a spatially developing initial-value solution.

For the special case of a potential mean swirl, the vortical modes are uncoupled from the acoustic modes, and their vorticity grows linearly as they propagate downstream. For a general vortical mean swirl the vorticity-dominated spatially developing disturbances can oscillate or amplify depending on the radial distribution of the mean swirl. The analysis clearly indicates a significant effect of the mean-flow swirl on the evolution of the incident disturbances.

Acknowledgments

The research was supported by the Office of Naval Research Grant N00014-92-J-1165 and monitored by L. Patrick Purtell. The authors would like to thank William K. Blake for his insightful comments.

References

[1] Atassi, H. M., "Unsteady Aerodynamics of Vortical Flows: Early and Recent Developments," *Aerodynamics and Aeroacoustics*, edited by K.-Y. Fung, World Scientific, Singapore, 1994, Ch. 4, pp. 121–172.

[2] Kerrebrock, J. L., "Small Disturbances in Turbomachine Annuli with Swirl," *AIAA Journal*, Vol. 15, No. 6, 1977, pp. 794–803.

[3] Golubev, V. V., and Atassi, H. M., "Sound Propagation in an Annular Duct with Mean Potential Swirling Flow," *Journal of Sound and Vibration*, Vol. 198, No. 5, 1996, pp. 601–616.

[4] Golubev, V. V., and Atassi, H. M., "Acoustic-Vorticity Waves in Swirling Flows," *Journal of Sound and Vibration*, Vol. 209, No. 2, 1998, pp. 203–222.

[5] Goldstein, M. E., "Unsteady Vortical and Entropic Distortions of Potential Flows Round Arbitrary Obstacles," *Journal of Fluid Mechanics*, Vol. 89, Pt. 3, 1978, pp. 433–468.

[6] Atassi, H. M., and Grzedzinski, J., "Unsteady Disturbances of Streaming Motions Around Bodies," *Journal of Fluid Mechanics*, Vol. 209, 1989, pp. 385–403.

[7] Cohen, H., Rogers, G. F. C., and Saravanamuttoo, H. I. H., *Gas Turbine Theory*, Longman Scientific and Technical, Essex, England, U.K., 1987, pp. 158, 159.

[8] Golubev, V. V., and Atassi, H. M., "Sound Propagation in Swirling Flows," *International Journal of Acoustics and Vibration*, Vol. 2, 1997, pp. 115–122.

[9] Howe, M. S., and Liu, J. T., "The Generation of Sound by Vorticity Waves in Swirling Duct Flows," *Journal of Fluid Mechanics*, Vol. 81, Pt. 2, 1977, pp. 369–383.

[10] Montgomery, M. D., and Verdon, J. M., "A Three-Dimensional Linearized Unsteady Euler Analysis for Turbomachinery Blade Rows," NASA CR-4770, March 1997.

[11] Tan, C. S., and Greitzer, E. M., "Nonaxisymmetric Compressible Swirling Flow in Turbomachine Annuli," *AIAA Journal*, Vol. 24, No. 1, 1986, pp. 92–100.

[12] Wundrow, D. W., "Small-Amplitude Disturbances in Turbomachine Flows with Swirl," NASA CR 195406, June 1994.

[13] Golubev, V. V., and Atassi, H. M., "Unsteady Swirling Flows in Annular Cascades, Part 2: Aerodynamic Blade Response," *AIAA Journal*, Vol. 38, No. 7, 2000, pp. 1150–1158.

S. Glegg
Associate Editor